

CHAPTER IV

RESULTS AND DISCUSSION

4.1 Rheological Characterization

The storage modulus (G') and loss modulus (G'') of polymers were measured by using the cone and plate rheometer. Figure 4.1 shows the plot of G' and G'' versus frequency of PS at 160°C. The strain amplitude used was 0.2% so that the rheological properties were in the viscoelastic range. Frequency range was between 0.01 to 100 rad/sec (transducer no.1, with 25 mm. cone and plate geometry).

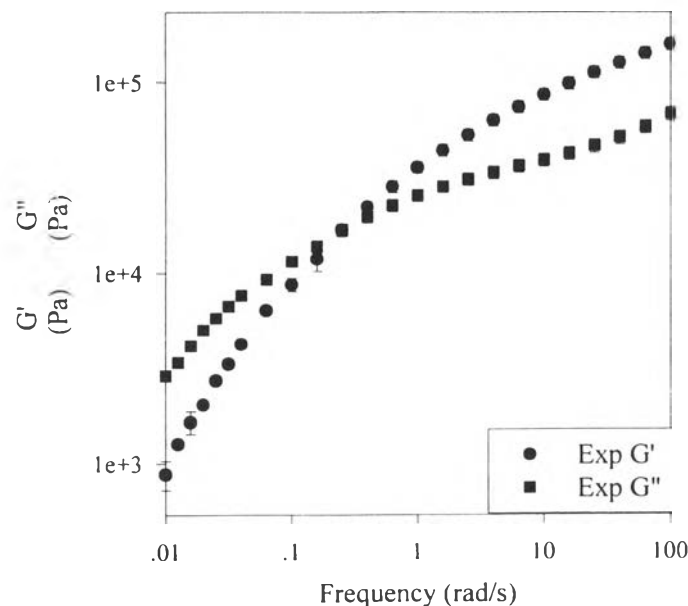


Figure 4.1 The storage modulus (G') and loss modulus (G'') of PS melt as a function of frequency at strain amplitude equal to 0.2% at 160°C.

Figures 4.2 – 4.4 show the storage modulus (G') and the loss modulus (G'') as functions of frequency (ω) of HDPE at 190°C . The strain amplitude used was 0.2% and frequency was varied between 0.01 to 100 rad/sec, using transducer no.1 and the 25 mm. cone and plate geometry. The liquid-like terminal zone was observed for all HDPE melts but the entanglement plateau zone was not found in this frequency range due to the frequency limitation of the instrument (100 rad/s).

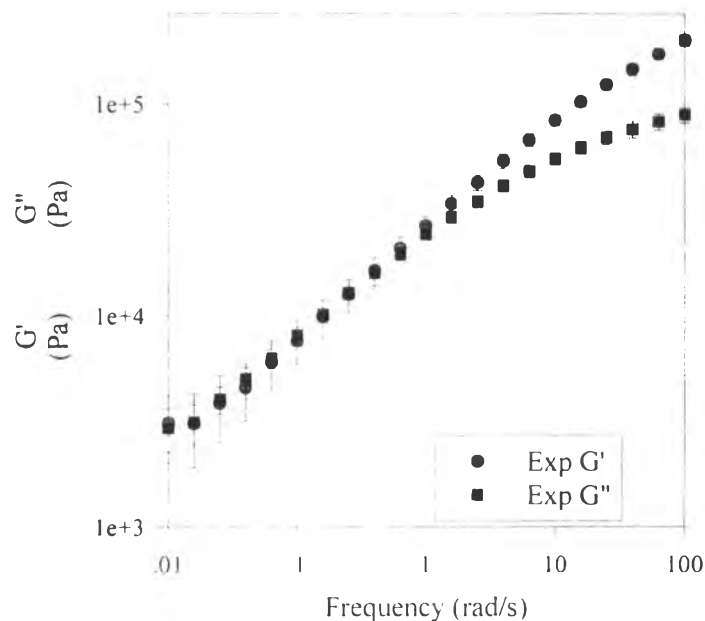


Figure 4.2 The storage modulus (G') and loss modulus (G'') of H5604F melt as a function of frequency at strain amplitude equal to 0.2% at 190°C .

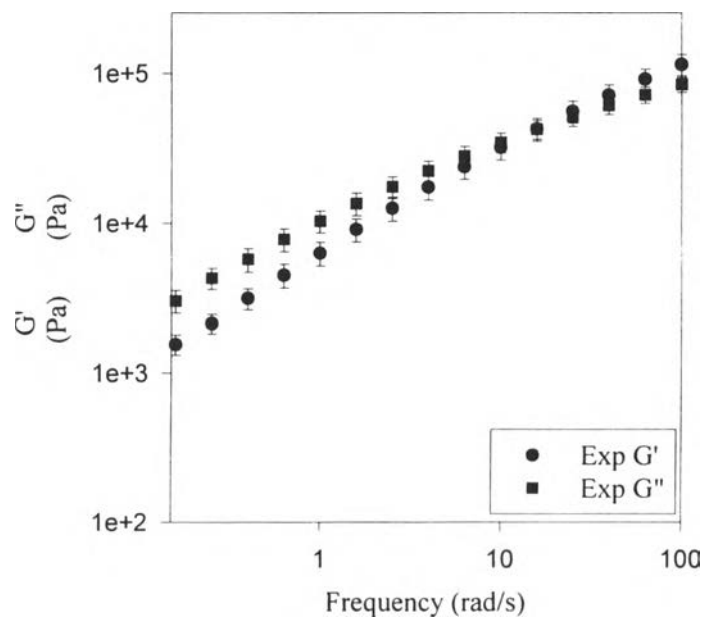


Figure 4.3 The storage modulus (G') and loss modulus (G'') of H5840B melt as a function of frequency at strain amplitude equal to 0.2% at 190°C.

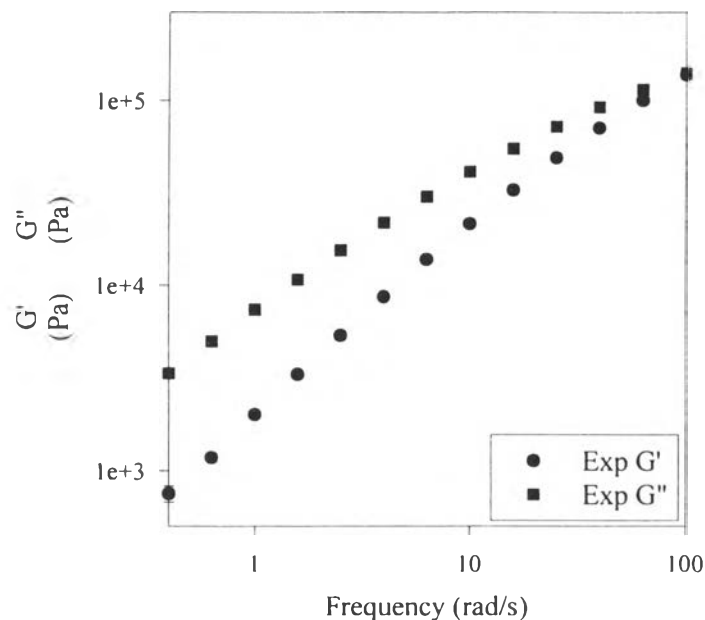


Figure 4.4 The storage modulus (G') and loss modulus (G'') of H5690S melt as a function of frequency at strain amplitude equal to 0.2% at 190°C.

Figures 4.5 – 4.7 show the storage modulus (G') and the loss modulus (G'') as a function of frequency (ω) of LDPE at 190°C. The strain amplitude used was 0.2% and frequency was varied between 0.01 to 100 rad/sec, using transducer no.1 and 25 mm. cone and plate geometry.

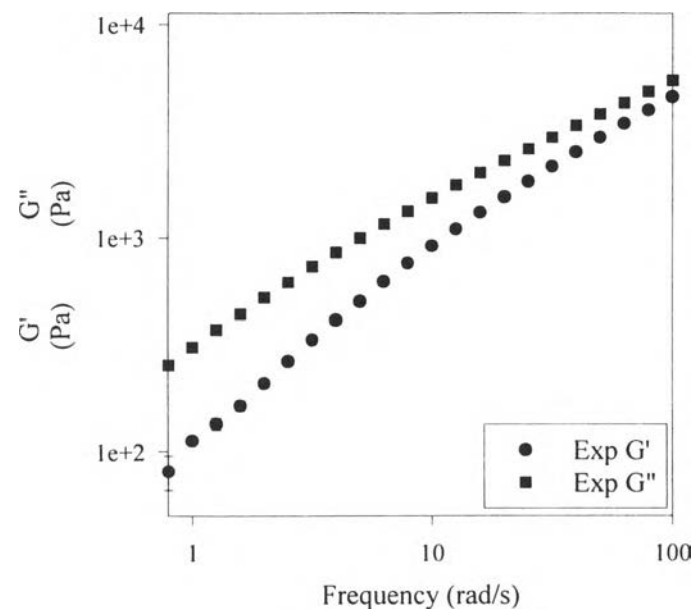


Figure 4.5 The storage modulus (G') and loss modulus (G'') of S1018 melt as a function of frequency at strain amplitude equal to 0.2% at 190°C.

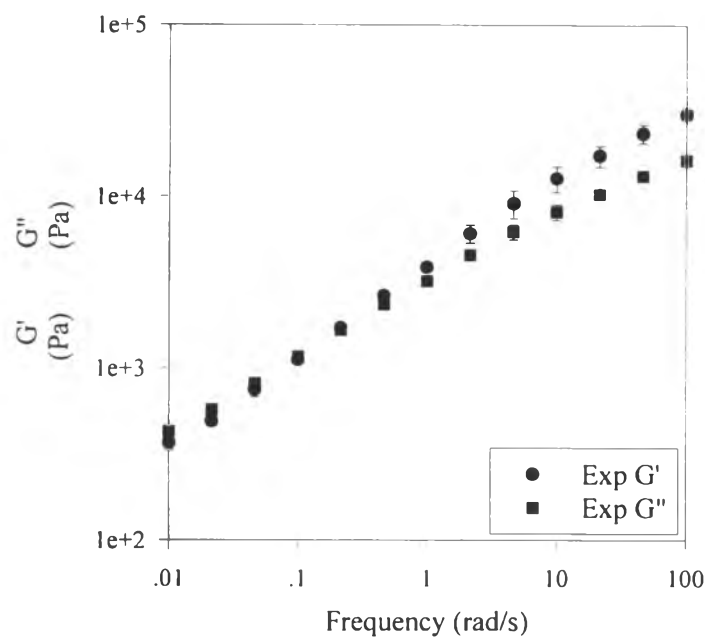


Figure 4.6 The storage modulus (G') and loss modulus (G'') of LD2130FA melt as a function of frequency at strain amplitude equal to 0.2% at 190°C.

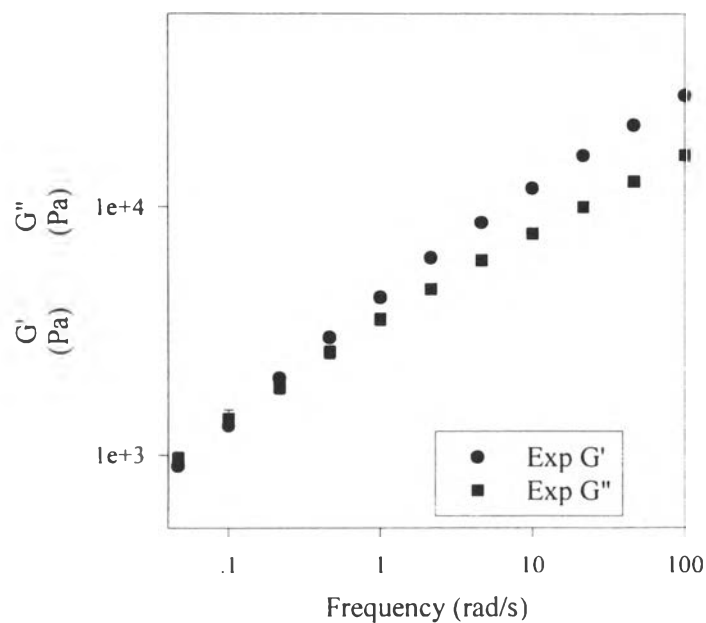


Figure 4.7 The storage modulus (G') and loss modulus (G'') of D2022 melt as a function of frequency at strain amplitude equal to 0.2% at 190°C.

4.2 Double Reptation Prediction

Figure 4.8 shows the comparison between the experimental data (G' and G'') and the prediction from the measured molecular weight distribution of PS by using the double reptation theory (Des Cloizeaux, 1988). The model parameter K was 1×10^{-18} sec and plateau modulus (G_N^0) was set equal 2×10^5 Pa. It is apparent that the double reptation theory provides a good agreement with the experimental data in the terminal regime but a very poor agreement in high frequency regime. The inaccuracy of the double reptation model in high frequency regime is due to lacks of contour-length fluctuation, dynamic dilution, and Rouse relaxation process (Pattamaprom *et al.*, 2000).

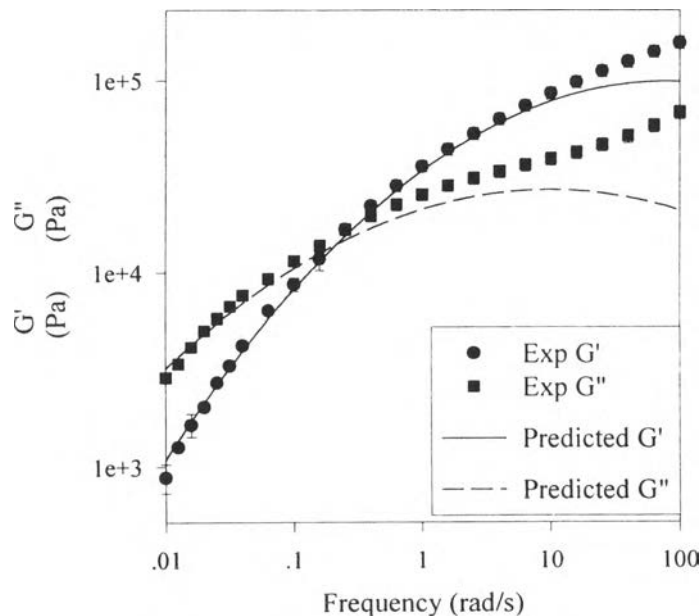


Figure 4.8 The comparison between the double reptation prediction of storage modulus, G' , and loss modulus, G'' , with experimental data for PS ($M_W = 2.3 \times 10^5$ and $M_n = 3.4 \times 10^4$) at 160°C .

Figures 4.9 – 4.11 show the comparison between the experimental data (G' and G'') and the prediction from the measured molecular weight distribution of HDPE by using the double reptation theory. The model parameter K was 6×10^{-18} sec and plateau modulus (G_N^0) was set equal to 2.6×10^6 Pa. We can see that the double reptation theory provides a good agreement with the experimental data in the frequency range between 1 – 100 rad/s. but a very poor agreement in the low frequency regime. The long-chain branching of HDPE is suggested to cause an inaccuracy of the double reptation model in the low frequency regime.

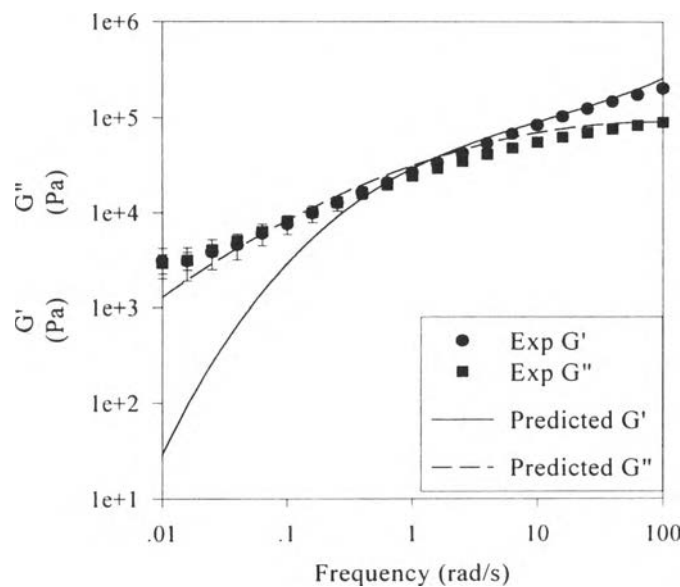


Figure 4.9 The comparison between the double reptation prediction of storage modulus, G' , and loss modulus, G'' , with experimental data for H5604F ($M_W = 4.9 \times 10^5$ and $M_n = 6.4 \times 10^2$) at 190°C .

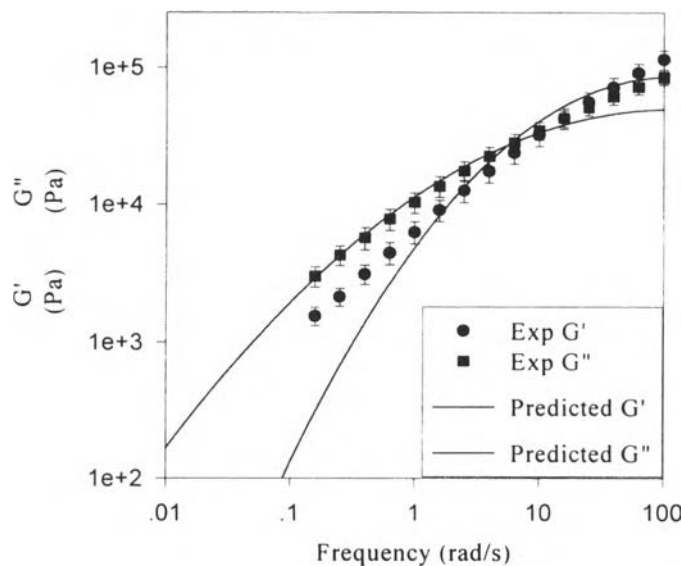


Figure 4.10 The comparison between the double reptation prediction of storage modulus, G' , and loss modulus, G'' , with experimental data for H5840B ($M_W = 4.7 \times 10^4$ and $M_n = 1.1 \times 10^3$) at 190°C .

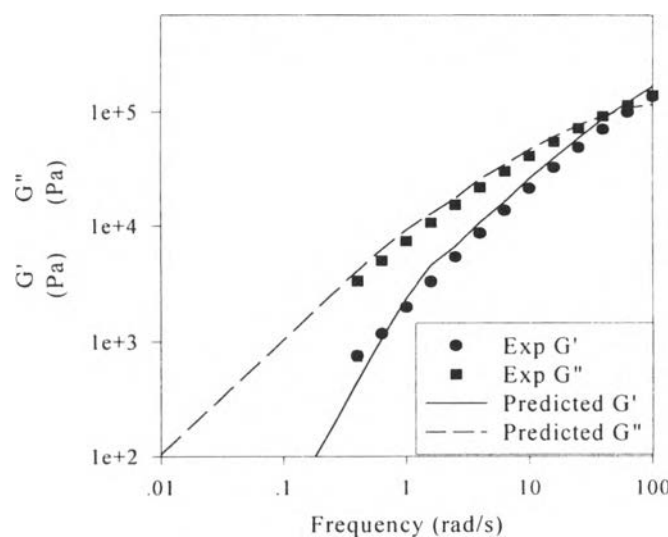


Figure 4.11 The comparison between the double reptation prediction of storage modulus, G' , and loss modulus, G'' , with experimental data for H5690S ($M_W = 4.5 \times 10^4$ and $M_n = 2.0 \times 10^3$) at 190°C .

Figure 4.12 – 4.14 show the comparison between the experimental data (G' and G'') and the prediction from the measured molecular weight distribution of LDPE by using the double reptation theory. The model parameter was $K = 1 \times 10^{-11}$ sec and plateau modulus (G_N^0) was set equal to 2.6×10^6 Pa. We can see that the double reptation theory fails in all ranges of frequency. The long-chain branching is suggested to cause an inaccuracy in the double reptation model, especially the higher degree of long-chain branching in LDPE is found to cause a large deviation in the prediction of rheological properties than those of HDPE.

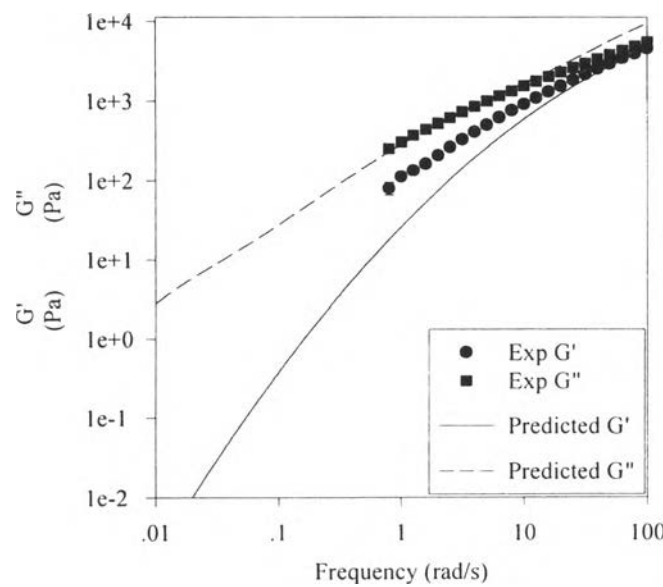


Figure 4.12 The comparison between the double reptation prediction of storage modulus, G' , and loss modulus, G'' , with experimental data for S1018 ($M_W = 7.2 \times 10^4$ and $M_n = 6.4 \times 10^2$) at 190°C.

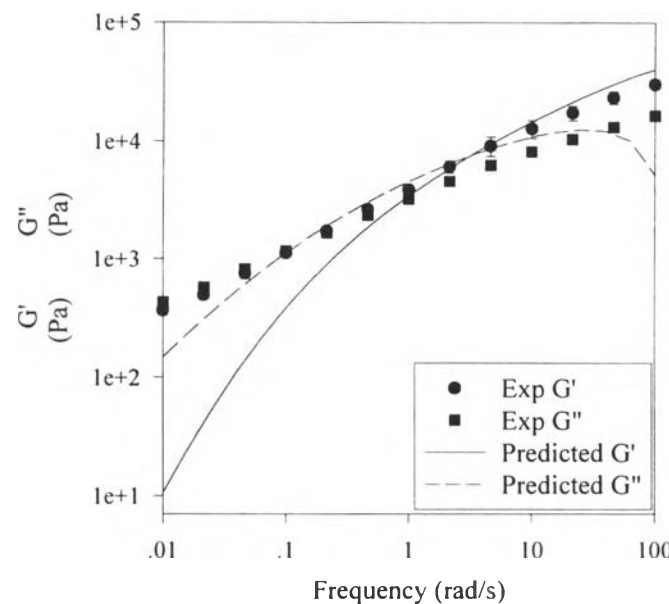


Figure 4.13 The comparison between the double reptation prediction of storage modulus, G' , and loss modulus, G'' , with experimental data for LD2130FA ($M_W = 5.4 \times 10^4$ and $M_n = 1.5 \times 10^2$) at 190°C.

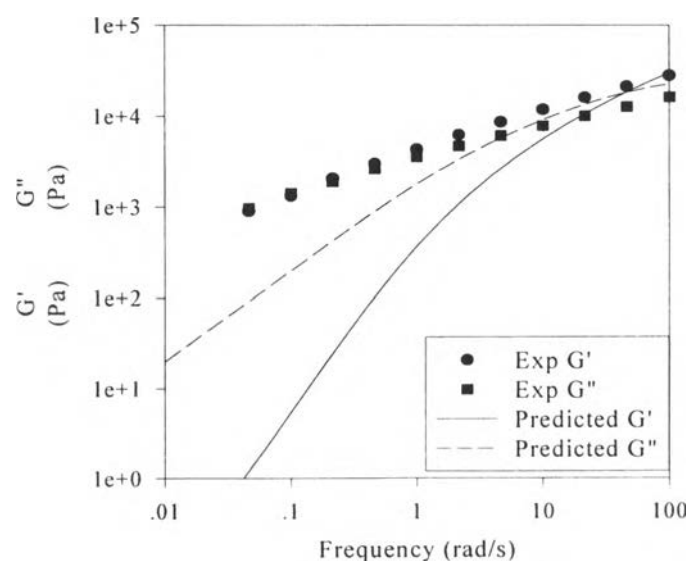


Figure 4.14 The comparison between the double reptation prediction of storage modulus, G' , and loss modulus, G'' , with experimental data for D2022 ($M_W = 1.1 \times 10^5$ and $M_n = 5.7 \times 10^3$) at 190°C.